PHILOSOPHICAL TRANSACTIONS OF THE ROYAL SOCIETY B

rstb.royalsocietypublishing.org

Research

Cite this article: Roháček K, Bertrand M, Moreau B, Jacquette B, Caplat C, Morant-Manceau A, Schoefs B. 2014 Relaxation of the non-photochemical chlorophyll fluorescence quenching in diatoms: kinetics, components and mechanisms. *Phil. Trans. R. Soc. B* **369**: 20130241. http://dx.doi.org/10.1098/rstb.2013.0241

One contribution of 20 to a Theme Issue 'Changing the light environment: chloroplast signalling and response mechanisms'.

Subject Areas:
cellular biology, biochemistry, biophysics, physiology

Keywords:
diatom, high light stress, photoprotection, photosynthesis, xanthophyll cycle, relaxation

Author for correspondence:
Benoît Schoefs
e-mail: benoit.schoefs@univ-lemans.fr

†These authors contributed equally to this study.

Electronic supplementary material is available at http://dx.doi.org/10.1098/rstb.2013.0241 or via http://rstb.royalsocietypublishing.org.

Royal Society Publishing

Relaxation of the non-photochemical chlorophyll fluorescence quenching in diatoms: kinetics, components and mechanisms

Karel Roháček[1,2,†], Martine Bertrand[3,†], Brigitte Moreau[2], Boris Jacquette[2], Christelle Caplat[4,5], Annick Morant-Manceau[2] and Benoît Schoefs[2]

[1]Biology Centre AS CR, p.r.i., IPMB, Branisovska 31, Ceske Budejovice 37005, Czech Republic
[2]MicroMar, Mer Molécules Santé, EA 2160, IUML FR – 3473 – CNRS, University of Le Mans, Avenue Olivier Messiaen, Le Mans Cedex 9 72085, France
[3]Le Cnam – SITI – CASER – MST – Microorganisms, Metals and Toxicity, BP 324, Cherbourg Cedex 50103, France
[4]ERPCB EA3914, IUT-UFR Sciences, Université de Caen, Boulevard du Maréchal Juin, Esplanade de la Paix, Caen 14032, France
[5]CORRODYS, Cherbourg-Octeville 50130, France

Diatoms are especially important microorganisms because they constitute the larger group of microalgae. To survive the constant variations of the light environment, diatoms have developed mechanisms aiming at the dissipation of excess energy, such as the xanthophyll cycle and the non-photochemical chlorophyll (Chl) fluorescence quenching. This contribution is dedicated to the relaxation of the latter process when the adverse conditions cease. An original nonlinear regression analysis of the relaxation of non-photochemical Chl fluorescence quenching, qN, in diatoms is presented. It was used to obtain experimental evidence for the existence of three time-resolved components in the diatom *Phaeodactylum tricornutum*: qNf, qNi and qNs. qNf (s time-scale) and qNs (h time-scale) are exponential in shape. By contrast, qNi (min time-scale) is of sigmoidal nature and is dominant among the three components. The application of metabolic inhibitors (dithiothreitol, ammonium chloride, cadmium and diphenyleneiodonium chloride) allowed the identification of the mechanisms on which each component mostly relies. qNi is linked to the relaxation of the ΔpH gradient and the reversal of the xanthophyll cycle. qNs quantifies the stage of photoinhibition caused by the high light exposure, qNf seems to reflect fast conformational changes within thylakoid membranes in the vicinity of the photosystem II complexes.

1. Introduction

Diatoms constitute the most dominant group of eukaryotic organisms in marine waters [1]. In marine ecosystems, diatoms play crucial roles in several biogeochemical cycles, including that of carbon [2]. It is estimated that diatom photosynthesis is responsible for up to 20% of the global primary production [3] and up to 40% of the carbon sequestered in the oceans [2]. This makes diatoms a major feeding source for other living organisms [2]. Thus, diatoms render tremendous ecological services, any of which is efficiently performed only when diatom fitness is preserved.

In marine ecosystems, the intensity of the environmental constraints is constantly modified [4,5]. For instance, turbulent water movements regularly expose microalgae to stresses such as high light (HL) conditions [6]. Regardless of their origin, stress conditions usually trigger a change in the equilibrium between the absorbed light energy and energy utilization [7], which ultimately results in lowering of primary productivity [8–11]. To minimize HL effects, microalgae have developed short- and long-term mechanisms to tune the balance between energy

utilization and dissipation. Carotenoids play crucial roles in these processes. Besides their protective function consisting of de-excitation of the chlorophyll (Chl) triplet state in the light-harvesting complex (LHC) antenna, the epoxidized xanthophylls, diadinoxanthin (Ddx) in diatoms, is involved in a dynamic, light-intensity-dependent short-term process of dissipation of excessive excitation energy into heat in the LHC, the xanthophyll cycle [7,12–14]. The de-epoxidation step is catalysed by lumen-localized enzymes, the so called Ddx de-epoxidases (DDEs) [13,14]. DDE binding to the thylakoid membranes is activated by the acidification of the thylakoid lumen, resulting from the establishment of the trans-thylakoidal pH gradient (ΔpH) under HL [15,16]. When the HL condition disappears, the stroma-located diatoxanthin (Dtx) epoxidase (DTE) catalyses Dtx expoxidation to Ddx [13,14]. Ascorbate and reduced nicotinamide adenine dinucleotide phosphate (NADPH) are the essential cofactors for de-epoxidase and epoxidase, respectively [13,14] (see electronic supplementary material, Data S1).

The dynamic dissipation as heat of the energy absorbed in excess is reflected in the quenching of Chl fluorescence and is referred as to non-photochemical quenching (NPQ) of Chl fluorescence [17,18], the intensity of which has been recently taken as a functional trait of the diversity of algae [13]. Very recently, the level of the specific LHC stress-related protein family, namely Lhcx, has been reported to be involved in NPQ [19]. In the diatom *Cyclotella meneghiniana*, NPQ comprises three components: (i) a rapid component (time-frame of tens of seconds) activated upon the transition from darkness to HL exposure, the intensity of which may be correlated with the amount of Dtx formed during the HL period; (ii) a medium component, major in amplitude, caused by the Dtx molecules formed through the xanthophyll cycle during HL treatment and (iii) a ΔpH-dependent and light-intensity-dependent slow component (several min time-frame), the intensity of which could be modulated by the Dtx amount present before HL treatment [20,21]. When the excessive incoming photon flux ceases, NPQ relaxes to its minimum [22]. Many reports have been dedicated to the kinetics of NPQ, whereas almost nothing is known about the processes involved in its relaxation.

In this contribution, an original method of nonlinear regression analysis of NPQ of the maximum variable Chl fluorescence yield (qN) relaxation kinetics is presented and used to elucidate the mechanisms on which the qN relaxation process relies. Metabolic inhibitors, such as dithiothreitol (DTT), ammonium chloride (NH_4Cl), cadmium (Cd) and diphenyleneiodonium chloride (DPI) were used to resolve the number of components, their kinetics and the mechanism on which they depend in the diatom *Phaeodactylum tricornutum*. A deep knowledge of the dissipation mechanisms of excess energy is of crucial importance for the understanding of diatom ecology and can certainly contribute to better exploitation of their capacity to produce high-value metabolites, the synthesis of which is enhanced under stress [23–25].

2. Material and methods

(a) Growth conditions

Phaeodactylum tricornutum UTEX 646 was grown in *f*/2 medium under a 16 L : 8 D regime and at 24 ± 1°C. Two other *P. tricornutum* strains: CCMP632 and NCC340, and *Odontella aurita* NCC86, *Entomoneis paludosa* NCC18.2, *Skeletonema costatum* NCC60, *Thalassiosira pseudonana* CCMP1335 and *T. weissflogii* NCC133 were cultured in artificial seawater [26] under the same light regime and at 16 ± 1°C. The different species were grown under cool-white fluorescent tubes (Philips TL-D 90, 36 W; photon flux density 300 µmol photons PAR m^{-2} s^{-1}) until the cultures reached the exponential growth phase, i.e. 4 days [27]. The irradiance was measured with a 4π waterproof probe (Walz, Germany) connected to a Li-Cor 189 quantum meter. Cell density was estimated either using the absorbance at 750 nm or by direct numbering using a Malassez haemotocytometer (microscope magnification 400×). Growth rate was calculated as $r = (\ln N_t - \ln N_0)/\Delta t$, where N_0 and N_t represent the cell density at time $t = 0$ and $t = t$, respectively, and Δt is the age of the culture (days).

(b) Chlorophyll fluorescence yield measurements

Chl fluorescence yield was monitored at the growth temperature after a dark-adaptation period (15 min). F_0 was recorded under a weak modulated light (less than 15 µmol PAR m^{-2} s^{-1}, 800 Hz). NPQ was induced during a 7 min non-saturating white actinic radiation (photon flux density 800 µmol PAR m^{-2} s^{-1}, KL 1500; H. Walz, Germany). At the end of the actinic illumination, the dark relaxation of the Chl fluorescence yield was recorded in order to allow quenching analysis. For each sample, the minimum (F_0, F'_0, F''_0), maximum (F_M, F'_M, F''_M) and maximum variable (F_V, F'_V, F''_V) Chl fluorescence yields in a dark-adapted state, in a light-adapted state and during the dark relaxation were measured, respectively [22] (see figure 1*a* for a representative recording). The slow Chl fluorescence induction kinetics were recorded using either a PAM 101–103 fluorometer (H. Walz, Germany) or an FMS1-modulated fluorometer (Hansatech Instruments, UK) [28].

DTT (final, 200 µM/stock, 20 mM), NH_4Cl (5 mM/1 M) and DPI (0.1–5 µM/2 mM) were diluted in distilled water or DMSO (DPI). For assays, the algae were incubated with the metabolic inhibitors 15 min before Chl fluorescence measurements (i.e. during the dark incubation) except for Cd (20 mg l^{-1}) that was present during the foregoing 24 h, as indicated in [27].

The intracellular Cd amount was determined as explained in the electronic supplementary material, Data S2.

To avoid CO_2 shortage during measurements, the cultures were provided with $NaHCO_3$ (final, 4 mM/stock, 0.2 M) [29]. Because the light intensity experienced by cells depends on cell density [30], the fluorescence measurements were performed using sample containing similar Chl amount as estimated by the absorbance at 665 nm (not shown).

(c) Pigment extraction and analysis

Pigment extraction and analysis by HPLC were performed as indicated in [31]. The de-epoxidation ratio (DER) was calculated as DER (%) = 100 [Dtx]/([Dtx] + 0.5[Ddx]).

(d) Oxygen evolution

Oxygen evolution measurements were performed as in [28]. Briefly, the oxygen was determined using a thermostated chamber equipped with a Clark-type oxygen electrode (DW2, Hansatech Instruments, UK). Oxygen evolution was

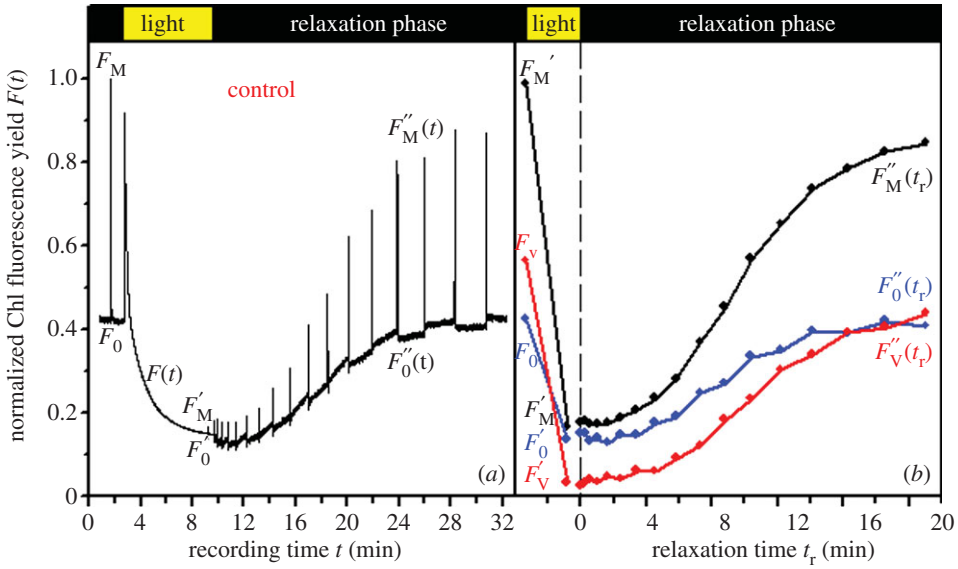

Figure 1. Slow fluorescence induction kinetics and input data for regression analysis. The representative slow Chl *a* fluorescence induction kinetics recorded on the control (non-treated) sample of *P. tricornutum* (*a*), and time courses of corresponding basic Chl fluorescence levels (*b*) used for resolution of components of the non-photochemical quenching of maximum *variable* Chl fluorescence yield (qN). Creation of qN takes place during an HL induction period (light) coming after the verification of the primary dark-adapted state (F_M, F_0). qN relaxation processes start from the light-adapted state (F'_M, F'_0) after switching the actinic light (800 μmol m^{-2} s^{-1}) off (vertical dashed line in *b*) and result in the course of dark-relaxation phase in renewal of the dark-adapted state. $F''_V(t_r)$ means the difference between $F''_M(t_r)$ and $F''_0(t_r)$ fluorescence levels for given time of dark relaxation (t_r). All data are normalized to F_M. For demonstration of stress influence on fluorescence induction kinetics, see the electronic supplementary material, figure S4-1. (Online version in colour.)

measured under actinic irradiance ranging from 0 to 2200 μmol photons PAR m^{-2} s^{-1}.

(e) Mathematical verification: statistics

The identical recording and processing of slow Chl fluorescence induction kinetics were assured by means of user-defined procedures. Data extracted from records were processed by the graphic software SigmaPlot 2000 for Windows (v. 6.10, SPSS, USA). Statistical verifications of calculations carried out by non-linear regression (fitting) procedures were evaluated by parameters R^2 and Norm. *R*, the coefficient of determination, measures how well a regression model describes the fitted data. 'Norm' stays for the square root of the sum of squares of the residuals. An R^2 value close to unity indicates that the relation between the independent and dependent variables is very well described by an entered regression equation. When the change in Norm value between two subsequent iterations is less than a given tolerance, the solution is considered to have been found.

Statistical significance of differences between corresponding pairs of data shown in graphs was found on the basis of the standard Student's *t*-test applied to individual unpaired or paired column data. The *t*-test determines whether the mean values of two data columns are significantly different by testing the hypothesis that the corresponding means are equal. The statistical significance ($p < 0.05$) is labelled by an asterisk. Results for $p > 0.05$ are not marked in graphs and are considered as statistically non-significant.

3. Results and discussion

(a) *Phaeodactylum tricornutum* is able to fully relax non-photochemical quenching

Figure 1*a* displays a typical slow Chl fluorescence induction kinetics recorded using non-treated *P. tricornutum*. Values of the maximum quantum yield of photosystem II (PSII) photochemistry (ϕ_{Po}) are close [27,28,32–34] or below the values reported in earlier studies [35]. The reasons for this discrepancy are not clear at present: it could result from the presence of a small pool of Dtx measured in the dark-adapted samples (data not shown, max 5%).

The high but non-saturating irradiation activated non-photochemical quenching as indicated by the low maximum Chl fluorescence yield reached at the end of the light phase (F'_M). As reported by Ruban *et al*. [36], the quenching intensity is three to five times larger (table 1) than that with higher plants [22]. As is frequently observed [27], F'_0 reached its minimum after approx. 3–5 min of actinic light exposure (figure 1*a*). The F'_0 value is lower than the F_0 level indicating that the processes involved in NPQ also affect the fluorescence yield of 'open' PSII reaction centres (figure 1*a*,*b*). Here, the real values of F'_0 can be slightly lower than the indicated values because of the presence of some remaining Q_A^- at the beginning of the relaxation phase [36]. After switching the actinic light off, NPQ relaxes (half-life more than 20 min; figure 1*b*). Similar values for the half-life of relaxation have been reported [33,37].

During this relaxation period, the fluorescence peaks result from a temporary closure of PSII reaction centres by short (0.8 s) saturation pulses applied to probe the maximum fluorescence yield (F''_M) in the absence of photochemical fluorescence quenching. During the relaxation period, the actual quantum yield of PSII photochemistry (ϕ_P) (for equations, see the electronic supplementary material, Data S3) increased regularly compared with the initial value of Φ_{Po} (figure 1*b*).

(b) qN relaxation kinetics in *Phaeodactylum tricornutum* are composed of three components

To characterize the components causing the dark-relaxation kinetics of qN, the nonlinear regression analysis proposed

Table 1. Effect of xenobiotics on the basic set of Chl fluorescence parameters, components of NPQ of Chl fluorescence (qN, qN_1) and DER. Statistical significance of resulted values found for given treatments compared with 'control' is $*p < 0.05$, $**p < 0.01$ and $***p < 0.001$. Means and corresponding standard deviations are the results of three to five samplings. For definitions and explanation of parameters summarized in this table, see the electronic supplementary material, Data S3 and S4.

parameter	control	+ DTT	+ NH_4Cl	+ Cd	+ Cd + DTT
Φ_{Po}	0.57 ± 0.01	0.56 ± 0.03	0.52 ± 0.01**	0.58 ± 0.03	0.53 ± 0.02*
qP	0.39 ± 0.05	0.35 ± 0.05	0.25 ± 0.04**	0.37 ± 0.08	0.28 ± 0.03*
qN	0.93 ± 0.02	0.89 ± 0.02*	0.75 ± 0.09**	0.93 ± 0.02	0.71 ± 0.07**
qN_1	0.95 ± 0.01[a]	0.91 ± 0.02*	0.95 ± 0.02	0.96 ± 0.01	0.85 ± 0.04**
q_0	0.68 ± 0.04	0.58 ± 0.04*	−0.15 ± 0.04***	0.65 ± 0.09	−0.0 ± 0.1***
Φ_{II}	0.08 ± 0.01	0.09 ± 0.01	0.05 ± 0.02*	0.07 ± 0.01*	0.07 ± 0.001**
NPQ	4.63 ± 0.73	3.12 ± 0.67*	0.47 ± 0.12***	4.67 ± 1.60	0.62 ± 0.28***
qNf	0.02 ± 0.01	0.04 ± 0.01*	0.30 ± 0.08***	0.04 ± 0.02	0.31 ± 0.07***
$\tau^f_{1/2}$ (s)	8.1 ± 3.1	23 ± 21	65 ± 38*	14.8 ± 2.6**	20.0 ± 4.5**
qNi	0.75 ± 0.09	0.67 ± 0.04	—	0.47 ± 0.09**	0.34 ± 0.20*
χ^1_0 (min)	8.9 ± 2.1	6.61 ± 0.35	—	17.0 ± 3.7**	4.25 ± 0.32*
qNs	0.18 ± 0.09[b]	0.20 ± 0.06	0.18 ± 0.03	—	0.20 ± 0.11
	—	—	0.47 ± 0.07[c]	0.45 ± 0.10	—
$\tau^s_{1/2}$ (min)	77 ± 31	58 ± 54	24 ± 16*	—	390 ± 490[d]
DER	62%	4.6%	5.1%	58%	5.2%

[a] $qN_1 = qNf + qNi + qNs$.
[b] The relaxing part of qNs.
[c] The non-relaxing ('permanent') part of qNs.
[d] A too large spread in values of $\tau^s_{1/2}$.

by Roháček [22] for higher plants was adapted to the case of diatoms. Owing to space limitations in this contribution, the mathematical reasoning is presented in the electronic supplementary material, Data S4. The procedure allows the fitting of the qN relaxation kinetics with three components (figure 2). This finding agrees with Grouneva *et al*. [20,38] who found that establishment of non-photochemical quenching consists of three components. The three components described here differ in their shape, half-life of relaxation and amplitude (table 1). The slow (qNs) and fast (qNf) components have exponential shapes while the intermediate and major component (qNi) is of sigmoidal shape (figure 2).

This shape can be explained by the difference in the rate of Dtx epoxidation and NPQ relaxation kinetics during the relaxation period (*C. meneghiniana* [39]; *P. tricornutum* [40]). Indeed, a sigmoidal relationship was found between the two parameters only in *P. tricornutum* [40]. The sigmoidal shape of the qNi component is not a peculiarity of *P. tricornutum* but has been found in each diatom species tested so far (see electronic supplementary material, Data S5).

(c) qNi relies on dissipation of the proton gradient and reversal of the xanthophyll cycle

The three components described in §3*b* reflect the pathways used by the photosynthetic apparatus to relax non-photochemical quenching after HL treatment. Grouneva *et al*. [20,38] found that the three components contribute to the establishment of NPQ. Therefore, we hypothesize that the three components described in this paper could be the counterparts of the pathways through which NPQ is established during actinic illumination. To test this hypothesis, a pharmacological approach was used to inhibit those pathways in the hope that the inhibitors would selectively affect either component. To this end, NH_4Cl a dissipator of ΔpH [41], was used. Representative kinetics obtained with each metabolic inhibitor are presented in the electronic supplementary material, Data S6.

In the presence of NH_4Cl, the F_V/F_M ratio (Φ_{Po}) was significantly reduced (table 1), confirming severe alterations of PSII functioning were induced by NH_4Cl [38], e.g. by inhibiting the oxygen evolving centre [42]. NH_4Cl slowed down the establishment of qN and NPQ (see electronic supplementary material, figure S6-1; table 1), but not that of qN_1, in which case the amplification of qNf compensated this effect, followed concurrently by the lowering of q_0 and the actual photochemical capacity of PSII (qP). NH_4Cl gave a very clear answer, as this uncoupler fully inhibited the intermediate and major component qNi as well as of Dtx formation (table 1). The Dtx found at the end of the light phase was already present at the end of the dark phase (data not shown). The absence of *de novo* Dtx formation was expected because Ddx de-epoxidation requires acidification of the thylakoid lumen, a phenomenon that NH_4Cl abolishes [41].

It is well established that Dtx formed through the operation of the xanthophyll cycle (see electronic supplementary material, Data S1) participates in process of non-photochemical quenching. To determine the contribution of the xanthophyll cycle to NPQ relaxation, the intensity of the different qN components was estimated in DTT-treated cells, DTT being an inhibitor of the Ddx de-epoxidase (see

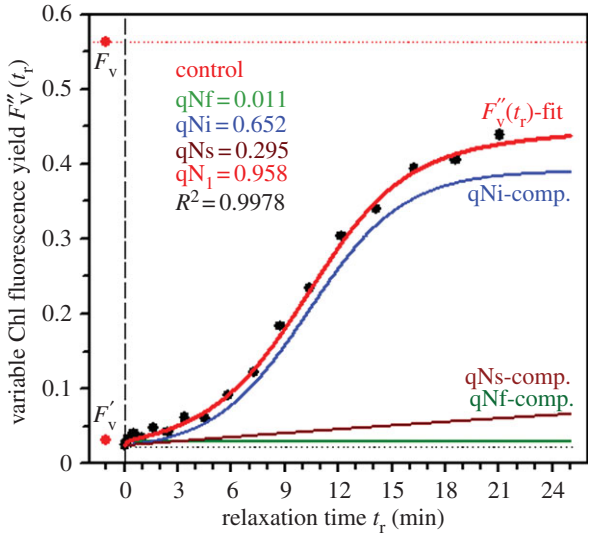

Figure 2. The relaxation kinetics of qN are composed of three components. Resolution of three qN components in the control sample (cf. figure 1) of *P. tricornutum* by the method of nonlinear regression analysis of experimental data is presented. Time courses of the maximum variable Chl fluorescence yield $F''_V(t_r)$ and actual magnitudes of three qN components are results of the fit according to equation S4-7 within the experimental data (black symbols). The input values of F_V, F'_V and $F''_V(1)$-level (black dotted line) applied to the fit procedure are highlighted together with the resulting numerical values for magnitudes of the fast (qNf), intermediate (qNi) and slow (qNs) components of the actual maximum NPQ (qN_1). The fit quality is demonstrated by squared value of the coefficient of determination (R^2). For experimental conditions, stated symbols and more details on the regression analysis, see the electronic supplementary material, Data S4. (Online version in colour.)

electronic supplementary material, Data S1). In the presence of DTT, the amplitude of qNi was *ca* 90% of the control value (table 1), demonstrating that the qNi relaxation component relies on dissipation of ΔpH and the reversal of the xanthophyll cycle. Consequently, qNi should be considered as the counterpart to the steady-state quenching component found in *C. meneghiniana* [37] and of qE in green algae and higher plants [43].

If the reasoning presented above is sound, the inhibition of the reversal of the xanthophyll cycle, i.e. the conversion of Dtx to Ddx, will affect the qN relaxation kinetics, especially qNi. To test this hypothesis, qN relaxation kinetics were recorded in the presence of Cd or DPI, two compounds reported to interact negatively with the reversal of the xanthophyll cycle (Cd [27]; DPI [44]).

Cd effects were similar to those reported in [27], i.e. (i) the DER reached in Cd-treated cells was 55% higher than that in control cells at the end of qN induction period (table 1) and (ii) qN relaxation was slower in the presence of Cd (table 1; electronic supplementary material, Data S6). In our conditions, the intracellular Cd concentration was around 3 fg $cell^{-1}$ (see electronic supplementary material, Data S7). Other works on *P. tricornutum* reported 10–30 fg $cell^{-1}$ [45–47]; for a review, see [4].

In the presence of Cd, the intensity of qNi was reduced to the same extent as the DER (table 1) and was slowed down, suggesting that Cd could directly interact with DTE (see electronic supplementary material, Data S1). An indirect effect of Cd could not be completely excluded, however, as Cd has been reported to interact with biochemical reactions generating NADPH, the cofactor of DTE [48–49] (see electronic supplementary material, Data S1). To obtain more information about the putative other target(s) of Cd, relaxation of NPQ was studied in Cd-treated cells incubated with DTT, an inhibitor of the forward reaction of the xanthophyll cycle and a chelator of Cd [43]. A synergistic effect of Cd and DTT resulted in a very similar impact on values of basic fluorescence parameters (see the electronic supplementary material, Data S3), as found for the NH_4Cl treatment.

DPI has been described as an inhibitor of the zeaxanthin epoxidase [44]. For very low DPI concentrations (less than 0.5 µM), qN remains unaffected (figure 3*a*,*c*). The progressive inhibition of the reversal of the xanthophyll cycle blocked the relaxation of qP, indicating that PSII reaction centres remained mostly closed when the xanthophyll cycle could not be reversed (data not shown). The amplitude of qNi progressively decreased while the DPI dose increased, and for the highest DPI concentration (5 µM) tested (figure 3*b*), the amplitude of qNi reached the minimum level close to zero, demonstrating the participation of the reversal of the xanthophyll cycle in qN relaxation (figure 3*c*).

Regardless of DPI concentration, qNf remained unaffected (figure 3*c*). As in Grouneva *et al.* [20,38], a small Dtx pool was detected before HL treatment. If such a pool is involved in the relaxation of qN, it is likely not available to Dtx epoxidase, as the DER calculated before actinic illumination and after the relaxation period were similar (data not shown). The increasing amount of DPI triggered a complementary increase in qNs to that of qNi; for a DPI concentration of 5 µM, qNs reached the maximum (figure 3*c*). The mechanism on which qNs relies remains obscure. qNs could reflect ΔpH dissipation as it has been shown that after Dtx has been activated, ΔpH is no longer needed for efficient NPQ [50]. It is also possible that in our conditions, diatoms may have experienced moderate photoinhibition because the value for the irradiance corresponding to the light saturating photosynthesis, E_k, was around 250 µmol photons PAR m^{-2} s^{-1} (see electronic supplementary material, Data S8). This value, however, is far from the HL level determined by Ting & Owens [30] as being fully photoinhibitory. More experiments have to be performed to clarify this point because in the presence of NH_4Cl, qNs was as intense as in the control but significantly accelerated (table 1). An interesting feature evidenced by the qN analyses presented in this contribution is the possibility that qNs becomes permanent (table 1 and figure 3*e*) i.e. its half-life cannot be measured. This was observed when the xanthophyll cycle was blocked by DTT and in the presence of Cd. The reasons for such a phenomenon remain unclear at present and may result from additional target(s) of DTT and Cd.

(d) The sigmoidicity of the qNi component is an intrinsic characteristic of ΔpH gradient relaxation in diatoms and reflects cooperative mechanisms

The results presented in this article establish that the component qNi is of sigmoidal shape (figure 2; electronic supplementary material, Data S5). In the presence of DTT, the kinetics of qNi remained sigmoidal, suggesting that this shape is linked to the establishment of ΔpH in diatoms. This reasoning fits with NPQ kinetics obtained from cells treated with *N*,*N*-dicyclohexylcarbodiimide (DCCD), an

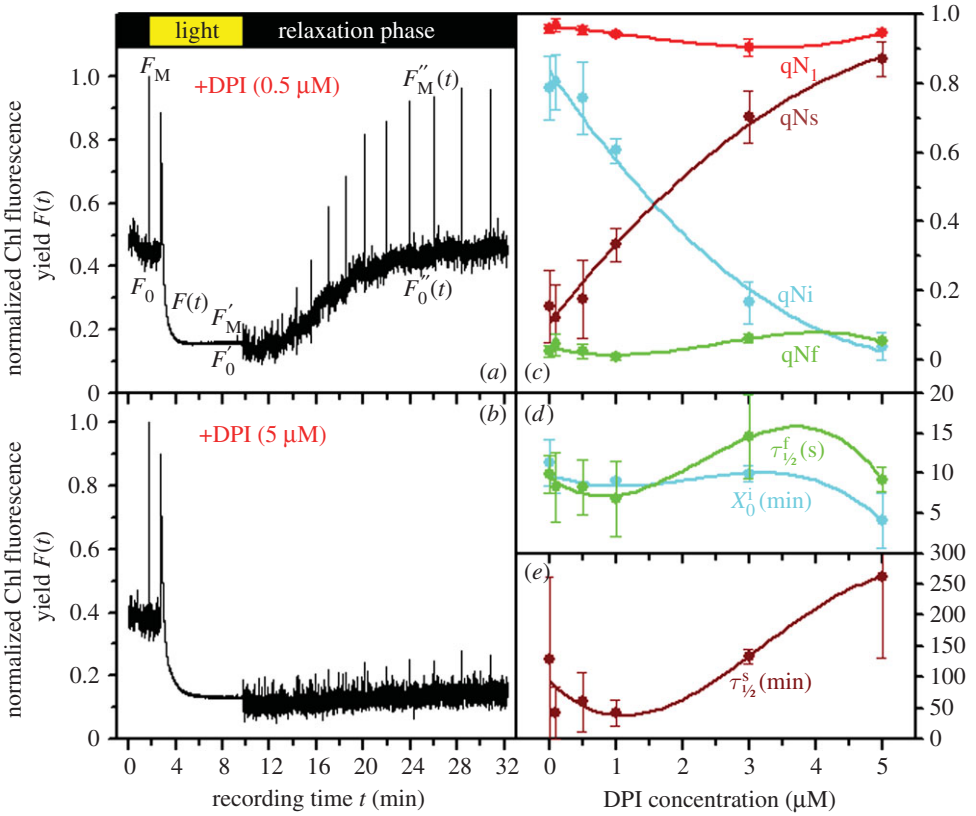

Figure 3. Effect of DPI on *P. tricornutum*. Influence of different concentrations of DPI (0 µM—control, 0.1, 0.5, 1, 3, 5 µM) on slow Chl fluorescence induction kinetics (*a*,*b*) and individual components of NPQ (*c*–*e*) of *P. tricornutum*. In comparison to the 'Control' (figure 1), a marked influence of DPI on the shape of induction kinetics was observed starting from 0.5 µM DPI (*a*) leading consecutively to activation of the strong inhibitory fluorescence quenching as seen for 5 µM DPI (*b*). This effect is reflected in the shape of qN components of NPQ (*c*) and their relaxation kinetics parameters (*d*,*e*) which are polynomial fits ($n = 3$) within experimental data (means of three repetitions and s.d. error bars are shown, relaxation parameters are expressed in seconds (s) or minutes (min), cf. table 1). For explanation of given parameters, see the electronic supplementary material, Data S4. (Online version in colour.)

inhibitor of ATP synthase [51,52]. In the presence of this chemical, protons were accumulated in the thylakoid lumen, triggering an intense pH gradient even under low-light illumination, which resulted in the development of NPQ. The kinetics of NPQ development recorded in these conditions are of sigmoidal shape [29]. Such a shape was not observed in the DCCD-treated green alga *Chlamydomonas* sp. ICE-L [53]. It has also been suggested that the activation of the quenching capacity of Dtx requires the protonation of special residues of the fucoxanthin chlorophyll proteins (FCPs) [29,36], which would result in a conformational change of the LHC. The quenching state of the LHC involves the binding of Dtx into hydrophobic regions of the protein and a dislocation of proton-binding domains, thereby establishing a stable NPQ that prevents fast relaxation of quenching in the absence of a bulk proton gradient. In higher plants, green algae and Prymnesiophyceae, the protonation of special amino acid residues of the LHCII resulting in LHCII aggregation could occur [54–56]. Aggregation of FCP could also happen in diatoms as suggested in [13,50]. Thus, the sigmoidal shape of the relaxation kinetics of the main component of NPQ would fit with a scenario starting with the deaggregation of FCPs, followed by the protonation of the special residues, reversing the conformational changes described above. Alternatively, and non-exclusively, the sigmoidal character could reflect the mode of action of the atypical member of the LHC stress-related protein family of diatoms, LHCX1, a protein serving as a molecular gauge in control of the level of NPQ [19,57].

4. Conclusion and perspectives

The kinetics of the relaxation of NPQ maximum variable fluorescence in diatoms result from the development of three individual components, qNf, qNi and qNs (figure 2). The kinetics of qNf and qNs follow an exponential curve, whereas that of qNi is sigmoidal in shape. This feature seems unique to diatoms. From the mechanism point of view, qNi relies on ΔpH relaxation and Dtx epoxidation. More experiments have to be performed to clarify the nature of the events involved in qNf and qNs. qNf could be related to a fast conformational change occurring within the thylakoid membranes at the start of the relaxation process. The different (very fast in their creation) qN components could be localized on PSII attached or detached LHCs [58]. The former would be related to the qN enhancing mechanism(s), whereas qNs could be heterogeneous from the mechanistic point of view and related to photoinhibition and/or partial dissipation of the pH gradient.

Acknowledgements. The authors warmly thank Ivana Hunalová (IPMB) and Sophie Hiard (University of Le Mans) for their efficient technical assistance. This article is dedicated to Dr Pavel Šiffel (23.11.1954–12.7.2003) and his wife Dr Gulmira Šiffelová (11.1.1959–12.7.2003), in memoriam, and as a token of our respect to their scientific work [59]. Dr Šiffel contributed to our early experiments developing a working protocol for fluorescence measurements on diatoms under heavy metal stress. His humour, scientific efforts and human qualities are unforgettable.

Funding statement. K.R. gratefully acknowledges the support by the Research Intent of IPMB AS CR (AV0Z50510513) and the University of Le Mans for an invited professor position.

References

1. Guiry MD. 2012 How many species of algae are there? *J. Phycol.* **48**, 1057–1063. (doi:10.1111/j.1529-8817.2012.01222.x)
2. Bowler C, Vardi A, Allen AE. 2010 Oceanographic and biogeochemical insights from diatom genomes. *Annu. Rev. Mar. Sci.* **2**, 333–363. (doi:10.1146/annurev-marine-120308-081051)
3. Field CB, Behrenfeld MJ, Dall'Osto L, Zito F, Bonente G, Falkowski G. 1998 Primary production of the biosphere: integrating terrestrial and oceanic components. *Science* **281**, 237–240. (doi:10.1126/science.281.5374.237)
4. Masmoudi S, Nguyen-Deroche N, Caruso A, Ayadi A, Morant-Manceau A, Tremblin G, Bertrand M, Schoefs B. 2013 Cadmium, copper, sodium and zinc effects on diatoms: from heaven to hell: a review. *Cryptogamie Algol.* **34**, 185–225. (doi:10.7872/crya.v34.iss2.2013.185)
5. Ewert M, Deming JW. 2013 Sea ice microorganisms: environmental constraints and extracellular responses. *Biology* **2**, 603–628. (doi:10.3390/biology2020603)
6. McIntyre HL, Kana TM, Geider RJ. 2000 The effect of water motion on short-term rates of photosynthesis by marine phytoplankton. *Trends Plant. Sci.* **5**, 12–17. (doi:10.1016/S1360-1385(99)01504-6)
7. Moulin P, Lemoine Y, Schoefs B. 2010 Modifications of the carotenoid metabolism in plastids: a response to stress conditions. In *Handbook of plant and crop stress* (ed. M Pessarakli), p. 407, 3rd edn. Boca Raton, FL: CRC Press.
8. Mus F, Toussaint JP, Cooksey KE, Fields MW, Gerlach R, Peyton BM, Carlson MP. 2013 Physiological and molecular analysis of carbon source supplementation and pH stress-induced lipid accumulation in the marine diatom *Phaeodactylum tricornutum*. *Appl. Microbiol. Biotechnol.* **97**, 3625–3642. (doi:10.1007/s00253-013-4747-7)
9. Sun GD, Mu M. 2013 Understanding variations and seasonal characteristics of net primary production under two types of climate change scenarios in China using the LPJ model. *Clim. Change* **120**, 755–769. (doi:10.1007/s10584–013–0833–1)
10. Thomas MK, Kremer CT, Klausmeier CA, Litchman E. 2012 A global pattern of thermal adaptation in marine phytoplankton. *Science* **338**, 1085–1088. (doi:10.1126/science.1224836)
11. Canion A, Mac Intyre HL, Phipps S. 2013 Short term to seasonal variability in factors driving primary productivity in a shallow estuary: implications for modelling production. *Estuar. Coast. Shelf Sci.* **131**, 224–234. (doi:10.1016/j.ecss.2013.07.009)
12. Szymanska R, Latowski D, Strzalka K. 2012 Chloroplasts: the powerful photoprotective machinery. *Curr. Chem. Biol.* **6**, 254–264.
13. Goss R, Jakob T. 2010 Regulation and function of xanthophyll cycle-dependent photoprotection in algae. *Photosynth. Res.* **106**, 103–122. (doi:10.1007/s11120-010-9536-x)
14. Bertrand M. 2010 Carotenoid biosynthesis in diatoms. *Photosynth. Res.* **106**, 89–102. (doi:10.1007/s11120-010-9589-x)
15. Lavaud J. 2007 Fast regulation of photosynthesis in diatoms: mechanism, evolution and ecophysiology. *Funct. Plant Sci. Biotechnol.* **1**, 267–287.
16. Jahns P, Latowski D, Strzalka K. 2009 Mechanisms and regulation of the violaxanthin cycle: the role of antenna proteins and membrane lipids. *Biochim. Biophys. Acta* **1787**, 3–14. (doi:10.1016/j.bbabio.2008.09.013)
17. Roháček K, Soukupová J, Barták M. 2008 Chlorophyll fluorescence: a wonderful tool to study plant physiology and plant stress. In *Plant cell compartments: selected topics* (ed. B Schoefs), p. 41. Kerala, India: Research Signpost.
18. Baker NR. 2009 Chlorophyll fluorescence of photosynthesis *in vivo*. *Annu. Rev. Plant Biol.* **59**, 89–113. (doi:10.1146/annurev.arplant.59.032607.092759)
19. Bailleul B *et al*. 2010 An atypical membre of the light harvesting complex stress-related protein family modulates diatom response to light. *Proc. Natl Acad. Sci. USA* **107**, 18 214–18 219. (doi:10.1073/pnas.1007703107)
20. Grouneva I, Jakob T, Wilhelm C, Goss R. 2008 A new multicomponent mechanism in the diatom *Cyclotella meneghiniana*. *Plant Cell Physiol.* **49**, 1217–1225. (doi:10.1093/pcp/pcn097)
21. Serôdio J, Lavaud J. 2011 A model describing the light response of the nonphotochemical quenching of chlorophyll fluorescence. *Photosynth. Res.* **108**, 61–76. (doi:10.1007/s11120-011-9654-0)
22. Roháček K. 2010 Method for resolution and quantification of components of the nonphotochemical quenching (q_N). *Photosynth. Res.* **105**, 101–113. (doi:10.1007/s11120-010-9564-6)
23. Lemoine Y, Schoefs B. 2010 Secondary ketocarotenoid astaxanthin biosynthesis in algae: a multifunctional response to stress. *Photosynth. Res.* **106**, 155–177. (doi:10.1007/s11120-010-9583-3)
24. Mimouni V, Ulmann L, Pasquiet V, Mathieu M, Picot L, Bougaran G, Cadoret JP, Morant-Manceau A, Schoefs B. 2012 The potential of microalgae for the production of bioactive molecules of pharmaceutical interest. *Curr. Pharm. Biotechnol.* **13**, 2733–2750. (doi:10.2174/138920112804724828)
25. Heydarizadeh P, Poirier I, Loizeau D, Ulmann L, Mimouni V, Schoefs B, Bertrand M. 2013 Plastids of marine phytoplankton produce bioactive pigments and lipids. *Mar. Drugs* **11**, 3425–3471. (doi:10.3390/md11093425)
26. Harrison PJ, Water RE, Taylor FJR. 1980 A broad spectrum artificial sea water medium for coastal and open ocean phytoplankton. *J. Phycol.* **16**, 28–35.
27. Bertrand M, Schoefs B, Siffel P, Roháček K, Molnar I. 2001 Cadmium inhibits epoxidation of diatoxanthin to diadinoxanthin in the xanthophyll cycle of the marine diatom *Phaeodactylum tricornutum*. *FEBS Lett.* **508**, 153–156. (doi:10.1016/S0014-5793(01)03050-2)
28. Nguyen-Deroche TLN, Caruso A, Le TT, Bui TV, Schoefs B, Tremblin G, Morant-Manceau A. 2012 Zinc affects differently growth, photosynthesis, antioxidant enzyme activities and phytochelatin synthase expression of four marine diatoms. *Scientific World Journal* **2012**, 982957. (doi:10.1100/2012/982957)
29. Lavaud J, Kroth P. 2006 In diatoms, the transthylakoid proton gradient regulates the photoprotective non-photochemical fluorescence quenching beyond its control on the xanthophyll cycle. *Plant Cell Physiol.* **47**, 1010–1016. (doi:10.1093/pcp/pcj058)
30. Ting CS, Owens TG. 1993 Photochemical and nonphotochemical quenching processes in the diatom *Phaeodactylum tricornutum*. *Plant Physiol.* **101**, 1323–1330.
31. Darko E, Schoefs B, Lemoine Y. 2000 An improved LC method for the analysis of photosynthetic pigments of higher plants. *J. Chromatogr.* **876A**, 111–116. (doi:10.1016/S0021-9673(00)00141-2)
32. Juneau P, Harrison PJ. 2005 Comparison by PAM fluorometry of photosynthetic activity of nine marine phytoplankton grown under identical conditions. *Photochem. Photobiol.* **81**, 649–653. (doi:10.1562/2005-01-13-RA-414.1)
33. Domingues N, Matos AR, Marques de la Silva J, Cartaxana P. 2012 Response of the diatom *Phaeodactylum tricornutum* to photoxidative stress resulting from high light exposure. *PLoS ONE* **7**, e38162. (doi:10.1371/journal.pone.0038162)
34. Jakob T, Schreiber U, Kirchesch V, Langner U, Wilhelm C. 2005 Estimation of chlorophjyll content and daily primary production of the major algal group by means of multiwavelength-excitation PAM chlorophyll fluorometry: performance and methodological limits. *Photosynth. Res.* **83**, 343–361. (doi:10.1007/s11120-005-1329-2)
35. Lavaud J, Rousseau R, van Gorkom HJ, Etienne AL. 2002 Influence of the diadinoxanthin pool size on photoprotection in the marine planktonic diatom *Phaeodactylum tricornutum*. *Plant Physiol.* **129**, 1398–1406. (doi:10.1104/pp.002014)
36. Ruban AV, Lavaud J, Rousseau B, Guglielmi G, Horton P, Etienne AL. 2004 The super-excess energy dissipation in diatom algae: comparative analysis with higher plants. *Photosynth. Res.* **82**, 165–175. (doi:10.1007/s11120-004-1456-1)
37. Eisenstadt D, Ohad I, Keren N, Kaplan A. 2008 Changes in the photosynthetic reaction centre II in the diatom *Phaeodactylum tricornutum* result in non-photochemical fluorescence quenching. *Environ. Microbiol.* **10**, 1997–2007. (doi:10.1111/j.1462-2920.2008.01616.x)
38. Grouneva I, Jakob T, Wilhelm C, Goss R. 2009 The regulation of xanthophyll cycle and non-photochemical fluorescence quenching by two alternative electron flows in the diatom

Phaeodactylum tricornutum and *Cyclotella meneghiniana*. *Biochem. Biophys. Acta* **1087**, 929–938. (doi:10.1016/j.bbabio.2009.02.004)

39. Grouneva I, Jakob T, Wilhelm C, Goss R. 2006 Influence of ascorbate and pH on the activity of the diatom xanthophyll cycle-enzyme diadinoxanthin de-epoxidase. *Physiol. Plant.* **126**, 205–211. (doi:10.1111/j.1399-3054.2006.00613.x)
40. Lavaud J, Rouseau B, Etienne A-L. 2002 In diatoms, a transthylakoid proton gradient alone is not sufficient to induce a non-photochemical fluorescence quenching. *FEBS Lett.* **523**, 163–166. (doi:10.1016/S0014-5793(02)02979-4)
41. Opanacenko VK, Vasyukhina LA, Naydov IA. 2010 Two types of ammonium uncoupling in pea chloroplasts. *Biochemistry* **75**, 784–791. (doi:10.1134/S0006297910060143)
42. Tsuno M, Suzuki H, Kondo T, Mino H, Noguchi T. 2011 Interaction and inhibitory effect of ammonium cation in the oxygen evolving center of photosystem II. *Biochemistry* **50**, 2506–2514. (doi:10.1021/bi101952g)
43. Müller P, Li XP, Niyogi KK. 2001 Non-photochemical quenching. A response to excess light energy. *Plant Physiol.* **125**, 1558–1566. (doi:10.1104/pp.125.4.1558)
44. Büch K, Stransky H, Hager A. 1995 FAD is a further cofactor of NAD(P)H and O_2-dependent zeaxanthin-epoxidases. *FEBS Lett.* **376**, 45–48. (doi:10.1016/0014-5793(95)01243-9)
45. Price NM, Morel FMN. 1990 Cadmium and cobalt substitution for zinc in a marine diatom. *Nature* **344**, 658–660. (doi:10.1038/344658a0)
46. Brembu T, Jorstad M, Winge P, Valle KC, Bones AM. 2011 Genome-wide profiling of responses to cadmium in the diatom *Phaeodactylum tricornutum*. *Environ. Sci. Technol.* **45**, 7640–7647. (doi:10.1021/es2002259)
47. Torres E, Cid A, Herrero C, Abalde J. 1998 Removal of cadmium ions by the marine diatom *Phaeodactylum tricornutum* Bohlin accumulation and long-term kinetics of uptake. *Bioresour. Technol.* **63**, 213–220. (doi:10.1016/S0960-8524(97)00143-0)
48. Groppa MD, Ianuzzo MP, Rosales EP, Vazquez SC, Benavides MP. 2012 Cadmium modulates NADPH oxidase activity and expression in sunflower leaves. *Biol. Plant.* **56**, 167–171. (doi:10.1007/s10535-012-0036-z)
49. Fagioni M, D'Amiel GM, Timperio AM, Zolla L. 2009 Proteomic analysis of multiprotein complexes in the thylakoid membrane upon cadmium treatment. *J. Proteome Res.* **8**, 310–326. (doi:10.1021/pr800507x)
50. Goss R, Pinto EA, Wilhelm C, Richter M. 2006 The importance of a highly active and ΔpH regulated diatoxanthin epoxidase for the regulation of the PS II antenna function in diadinoxanthin cycle containing algae. *J. Plant Physiol.* **163**, 1008–1021. (doi:10.1016/j.jplph.2005.09.008)
51. McCarty RE, Rachter E. 1967 The inhibition and stimulation of photophosphorylation by *N,N′*-dicyclohexylcarbodiimide. *J. Biol. Chem.* **242**, 3435–3439.
52. Shoshan V, Selman BR. 1967 The interaction of *N,N′*-dicyclohexylcarbodiimide with chloroplast coupling factor 1. *J. Biol. Chem.* **255**, 384–389.
53. Mou S, Zhang X, Ye N, Miao J, Cao S, Xu D, Fan X, An M. 2013 Analysis of ΔpH and the xanthophyll cycle in NPQ of the Antartic sea ice alga *Chlamydomonas* sp. ICE-L. *Extremophiles* **17**, 477–484. (doi:10.1007/s00792-013-0532-x)
54. Horton P, Ruban AV, Rees D, Pascal AA, Noctor G, Young AJ. 1991 Control of the light-harvesting function of chloroplast membranes by aggregation of the LHCII chlorophyll-protein complex. *FEBS Lett.* **292**, 1–4. (doi:10.1016/0014-5793(91)80819-0)
55. Goss R, Garab G. 2001 Non-photochemical chlorophyll fluorescence quenching and structural rearrangements induced by low pH in intact cells of *Chlorella fusca* (Chlorophyceae) and *Mantoniella squamata* (Prasinophyceae). *Photosynth. Res.* **67**, 185–197. (doi:10.1023/A:1010681511105)
56. Walters RG, Ruban AV, Horton P. 1994 Higher plant light harvesting complexes LHCIIa and LHCIIc are bound by dicyclohexylcarbodiimide during inhibition of energy dissipation. *Eur. J. Biochem.* **226**, 1063–1069. (doi:10.1111/j.1432-1033.1994.01063.x)
57. Lepetit B, Goss R, Jakob T, Wilhelm C. 2011 Molecular dynamics of the diatom thylakoid membrane under different light conditions. *Photosynth. Res.* **111**, 245–257. (doi:10.1007/s11120-011-9633-5)
58. Miloslavina Y, Grouneva I, Lambrev PH, Lepetit B, Goss R, Wilhelm C, Holzwarth AR. 2009 Ultrafast fluorescence study on the location and mechanism of non-photochemical quenching in diatoms. *Biochim. Biophys. Acta* **1787**, 1189–1197. (doi:10.1016/j.bbabio.2009.05.012)
59. Květoň J, Durchan M, Roháček K, Šantrůček J, Vácha F, Šesták Z. 2005 PAVEL ŠIFFEL (1954–2003) or life full of chlorophyll. *Photosynthetica* **43**, 323–328. (doi:10.1007/s11099-005-0055-5)